

Accurate 3D surface measurement of mountain slopes through a fully automated image-based technique

Mattia Previtali • Luigi Barazzetti • Marco Scaioni

Received: 28 November 2013 / Accepted: 24 March 2014 / Published online: 10 April 2014

Introduction

The geometric modeling of rock slopes is an essential aspect for several geological and geotechnical analyses. First of all, an adequate model can be used for the evaluation of risk scenarios, e.g., by using a trajectographic analysis (Agliardi and Crosta 2003) or for the localization of discontinuities (Slob et al. 2005; Ferrero et al. 2009). Secondly, the knowledge of local topography may be exploited to optimize the design of reinforcement or protection structures (Duncan and Norman 1996; Scaioni et al. 2010). Eventually, the comparison between 3D geometric models gathered at different times might help detect and evaluate existing failure processes, like rock falls (Abellán et al. 2006; 2009; Oppikofer et al. 2009), soil weathering (Travelletti et al. 2008) or landslides (Prokop and Panholzer 2009; Kasperski et al. 2010; Nguyen et al. 2011). The acquisition of a 3D geometric model of a slope can be pursued by different techniques. These could be categorized according to different criteria, for example on the basis of the sensor's platforms: (i) *spaceborne* (high-resolution satellite sensors); (ii) *airborne* (fixed wing aircrafts, helicopters, Un-manned Aerial Systems); and (iii) *ground-based* (or *terrestrial*) instruments. The selection of the adopted platform mainly depends upon the spatial extension of the area to investigate, the required resolution and accuracy of the geometric model, and the site accessibility. Consequently, spaceborne platforms can be used when 3D models of large

M. Previtali (✉) • L. Barazzetti
Politecnico di Milano, Department of Architecture, Built Environment and Construction Engineering, Via Ponzio 31, 20133 Milano, Italy
e-mail: mattia.previtali@polimi.it

L. Barazzetti
e-mail: luigi.barazzetti@polimi.it

M. Scaioni
Tongji University, College of Surveying and Geo-Informatics, Center for Spatial Information Science and Sustainable Development Applications, 1239 Siping Road, 200092 Shanghai, Peoples Republic of China
e-mail: marco@tongji.edu.cn

areas are needed. Indeed, resolution and accuracy of such models is usually in the order of a few meters (Joyce et al. 2009; Martha et al. 2010). Airborne platforms incorporating photogrammetric cameras (Kraus 2007) and/or LiDAR sensors (Heritage and Large, 2009) allow for a high productivity and results are those typical of topographic maps. However, because sensors are generally mounted on the bottom side of the aircraft and look downwards, the field-of-view is limited to the nadir direction. Thus these platforms are not adequate for surveying vertical or sub-vertical rock faces. Unmanned Aerial Systems (UAS) (Eisenbeiss and Sauerbier 2011; Nex and Remondino 2014) equipped with different sensors (mainly digital cameras) allows for a higher flexibility in data acquisition giving the chance to improve the performances over vertical regions. However, in the case of vertical cliffs, approaches based on ground-based sensors (iii) are the most suitable. This group of techniques, which mainly entails theodolite-based surveying, digital photogrammetry and terrestrial laser scanning (TLS), may offers a better view of the rock face scene and also may shorten the distance between sensor and target, with a consequent increment of resolution and precision. The main factor limiting the use of terrestrial platforms is that all the required instrumentation has to be carried in front of the site to be surveyed.

For the sake of completeness also real-time *Global Navigation Satellite Systems*–GNSS have been used in some specific applications (Abidin et al. 2007; Gao et al. 2011) but with a low productivity and the need of directly access the slope to be surveyed.

Theodolite surveying (Feng et al. 2001; Barla et al. 2010; Yang et al. 2007) is a traditional and well assessed technique for measuring points on the ground surface (Schofield and Breach 2007). Nowadays, high-end instruments may provide $\pm 0.5''$ angle precision and ± 0.6 mm distance precision when using phase-difference measurements and topographic reflectors. Precision drops down to $\pm 2.0\div 3.0$ mm when natural points are measured instead of using reflectors. Within *robotic total stations*, data acquisition can be automatically scheduled at nodes of a regular grid. This option makes a theodolite very close to a terrestrial laser scanner, although it is largely slower. Even if theodolites may achieve a high precision and accuracy, the acquisition range is limited to a few hundred meters. Furthermore, the level of automation is still low and data acquisition must be completely accomplished in the field, i.e., there is not chance to recover further information at the post-processing stage.

A *terrestrial laser scanner* can be considered as an evolution of a theodolite (see Shan and Toth 2009; Vosselman and Maas, 2010). Roughly speaking, scanning is obtained using a rotating mirror system deviating the laser pulses emitted by a rangefinder towards the target surface. When the emitted signal encounters an obstacle, the pulse is reflected back allowing the range measurement. The user does not perform

any point collimation, but has to define the scan window only. Two different range measurement principles are used: phase-shift or Time-of-Flight (ToF). The principal differences between both are precision, data acquisition speed and maximum distance allowed. Phase-shift measures have maximum measurement range of 50–100 m, precision of a few millimeters, acquisition speed in the order of $10^5\text{--}10^6$ Hz. ToF scanner measurements are used for long range applications, up to 6 km for high reflectivity surfaces, but have a lower precision (few centimeters) and lower acquisition speed $10^4\text{--}10^5$ Hz. Angular scanning resolution, in the order of 50 μrad , allows a very high sampling density, resulting in million points measured on the object surface, in relatively short time. In recent years TLS has been really successful for geological and topographical applications (Jaboyedoff et al. 2012; Pirotti et al. 2013a). This is due to the straightforward acquisition of 3D points, the simplicity of registration also in case of multiple scans, and the capability of gathering a dense point cloud independently from the texture of the slope. The availability in the latest years of instruments with full-waveform operational mode (Pirotti et al. 2013b) allows the acquisition of the bare rock also in those areas partially covered by vegetation.

Photogrammetry allows the reconstruction of the surface of an object based on at least two images which depict it from different points of view (Kraus 2007). The use of such approach presents some undoubtable advantages with respect to other techniques: (i) the possibility of surveying inaccessible areas, as for instance tall rock faces; (ii) the reduced time for the acquisition of primary data (imagery); (iii) the low cost of the instrumentation; (iv) no need for skilled operators in the data acquisition stage; and (v) the opportunity to use the same camera body, with diverse lenses, for different objects. However, photogrammetry had a limited use for rock face survey in the past and only recently the research activity turned out to focus on this topic (Mora et al. 2003; Salvini et al. 2011).

Image analysis or photogrammetric methods were developed by different authors to evaluate the stability of rock faces. In many cases, the principal goal is the extraction and mapping of discontinuities in the rock, complementary or as an alternative to a traditional compass-based survey (Reid and Harrison 2000; Lemy and Hadjigeorgiou 2003; Kemeny and Post 2003). There are also some commercial software packages, developed in particular for open mine and underground excavation surveys (Siriovision®, Shapematrix3D®, 3DM Analyst®) that are able to extract 3D models and discontinuities in rock faces. Even if these software packages are based on image processing, they are not thought for photogrammetric purposes. In some software packages the algorithms for camera calibration are not implemented and in general no more than a pair of stereo-images can be processed at once, limiting the extension of the area to analyze and increasing the project complexity. Indeed, for covering large areas several partial models are merged together to obtain the overall 3D

reconstruction. However, the union of different models generates some errors and requires more time to accomplish the full process.

In the last decades the technological development of digital cameras and the uprising computer performances have stimulated different authors to develop automatic methods for model generation based on the use of digital images (Furukawa and Ponce 2007; Agarwal et al. 2009). However, these implementations are not thought for slope surveying and monitoring where both accuracy aspects and statistical analysis of results play an important role. In this paper, the authors would highlight which is the current potentiality of image-based 3D reconstruction techniques for mountain slope modelling, and to address future research and software development. In order to exemplify this process, a photogrammetric procedure which has been developed by the authors to this purpose is presented and discussed in the following.

The presented methodology does not automatically extract discontinuities planes. In fact, the target was to develop a tool for accurate three-dimensional geometric representation of slopes and rock cliffs. Given a 3D model, and particularly a 3D point cloud, manual or automatic extraction of discontinuities can be performed at a later stage using one of the approaches presented in literature (García-Sellés et al. 2011; Gigli and Casagli 2011; Longoni et al. 2012).

The outline of the paper is as follows: Section 2 illustrates the photogrammetric methodology that has been developed and highlights challenges for its full automation. Section 3 presents some results achieved in field experiments and comparisons with other sensors or commercial software packages. In Section 4 some final conclusions are drawn.

The photogrammetric reconstruction of rock slopes

The photogrammetric pipeline for surface reconstruction

gives the possibility of determining the 3D coordinates of points from stereo or multiple images (i.e., from images of the same object captured from different points of view (Luhmann 2011)). The photogrammetric process is quite complex, due to the need of extracting 3D information from 2D imagery. On the other hand, the use of digital cameras in conjunction with the increased computational capability of computers can be exploited to obtain the reconstruction of 3D surfaces in a comparable way with respect to laser scanning techniques.

Broadly speaking, the standard photogrammetric process in close-range applications is based on four main steps. First of all, each camera needs *calibration* (Fraser 2013), which is finalized to setup a reference system on each image to enable image coordinate measurement and to compensate for lens distortions. This turns out in the computation of the *principal distance*, the *principal point* position, and a set of *additional*

parameters (AP's) for modeling lens distortion according to one of the available models. Calibration is periodically performed by using a test field, and although the user has to acquire a small block of pictures (usually 10–16), the process is fully automated today. In the applications shown in this paper, diverse amateur SLR cameras have been used after calibration (see Table 1).

The second step consists in *data acquisition*. Although it involves less theoretical aspects than other tasks, its relevance to the quality of the final output is higher than it is usually thought. Indeed, the geometry of the image acquisition is fundamental for successful image orientation and surface reconstruction stages. In fact, every application requires a tailored surveying planning, as can be seen in the examples reported in Section 3. Although there are specific techniques for photogrammetric network design (Fraser 2013), generally this is planned based on some tips, on general best practices, and on the expertise of the operators. The major aspects to be considered in the planning phase are: camera-to-target distance, focal length, adequate overlap among images, and some external constraints for geo-referencing the image block (e.g., some *ground control points*—GCP's—having known coordinates in the ground reference system—GRS).

The third task is *image orientation*, which allows the reconstruction of the *exterior orientation* (EO) of any image, i.e., the camera spatial position and rotation with respect to the GRS. This determination is pursued by identifying the same points (called 'homologous' or 'tie' points) in different images, whose image coordinates are accurately measured. In the image formation process it is generally assumed that the object point, the corresponding image point and the perspective center of an image are aligned (Kraus 2007). Such *collinearity constraint* is exploited to setup a system of equations where the measured image coordinates are the observed quantities, while the EO parameters and the 'object' coordinates (in the GRS) of tie points are the unknowns to compute. The system is typically redundant to overcome the presence of measurement errors. This implies the use of Least Squares (LS) method for the estimation of the solution and its precision. External constraints (e.g., GNSS/INS data, Ground Control Points—GCP's) can be efficiently incorporated into the solution in order to define the 3D *datum* and to limit the errors due to block instability. Indeed, in a system where observations are image coordinates only, the reconstruction is affected by an overall ambiguity consisting in a seven parameter similarity transformation. By adding external constraints the 'datum problem' can be solved. Moreover, sometimes a block of images may feature a weak geometry due to the large size, poor image overlap, presence of sub-block partially disconnected among them. In such cases, the effect of measurement errors on the estimated EO parameters and point coordinates are emphasized. Such condition of block instability may be overcome by adding some GGC's.

Table 1 Calibration parameters and sensor characteristics for the cameras used in the experimental applications

	Nikon D80 Sigma 20 mm lens	Nikon D700 Tamron 180 mm lens	NIKON D700 Tamron 90 mm lens
Principal distance (mm)	20.8638	180.00	90.00
Image size (pixel)	3,872 × 2,592	4,256 × 2,832	4,256 × 2,832
Format size (mm)	23.6192 × 15.8112	36.00 × 23.9549	36.00 × 23.9549
Sensor type	CCD	CMOS	CMOS

Traditionally, recognition of homologous points in images is performed manually. This operation is time-consuming and sometimes difficult to be accomplished owing to the poor image texture. Rock slopes are typical cases where this problem may occur. In some applications where some targets can be positioned on the object, they can be used as homologous points and automatically detected by using recognition algorithms (Fraser and Cronk 2009). However, the possibility of fully automatic target-less orientation of close-range blocks is now possible in the most applications (Barazzetti et al. 2011; Pierrot Deseilligny and Clery 2011). The automation of image orientation simplifies the photogrammetric process and reduces the cost in term of man work. Examples reported in Section 3 have been worked out by using the software ATiPE (Barazzetti et al. 2010). A similar workflow has been recently included in some commercial photogrammetric software packages (e.g., PhotoModeler® 2013, Asigoft Photoscan®) that may be used as a commercial alternative to ATiPE.

Once EO of images are defined it is possible to extract a dense (in terms of distance between adjacent points) point cloud from the images (fourth step). The use of *Area Based Matching* (ABM) algorithms allows one to reconstruct the slope surface in automatic way, this time starting from the computed EO parameters. All matching techniques belonging to this category look for corresponding areas on different images. In particular the fundamental hypothesis is that points belonging to different images are homologous if the intensity level in their neighborhood is similar. This is a strong hypothesis that in many cases may not be fulfilled due to variation of

light conditions, significant perspective deformations, etc. The various matching techniques differ in the way they try to avoid mismatches. In the next paragraph we will focus on MGCM+technique implemented in this work for the reconstruction of rock faces. After image matching, a point cloud of the whole surface is available. Thanks to the knowledge of the EO of each camera station, the reconstructions coming from different sub-groups of images are already referred into the same GRS.

MGCM+matching algorithm

Different automatic matching techniques were developed in the last decades both in Photogrammetry and Computer Vision (Grün 2012). In photogrammetry a well-known automatic matching technique is *LS Matching* (LSM) proposed by Grün (1985). In traditional LSM the similarity of points in two images is evaluated on the basis of intensity values of neighbor pixels. A candidate point on the reference image is sought on a second image ('slave'), where its approximate position is computed thanks to known EO parameters and to a rough 3D model of the object. As the same object is depicted in different ways on both images, LSM incorporates approximate models to compensate for both geometric and radiometric deformations. Estimation of transformations' parameters is carried out through LS after linearization. The high performance of this algorithm is its adaptivity, i.e., it can find correspondences also in case of limited perspective deformations in two images, unlike the well-known *Normalized Cross Correlation*

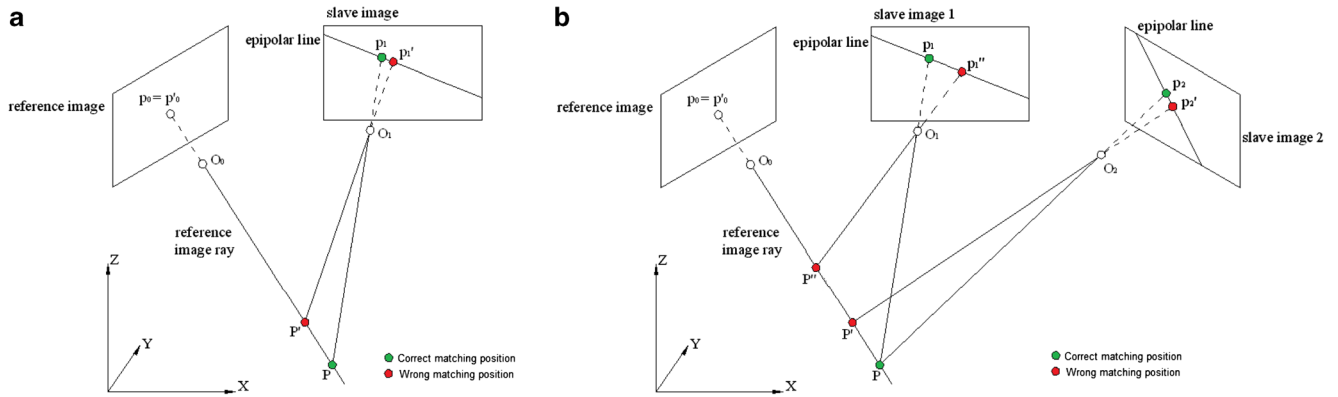


Fig. 1 Ambiguous intersection of a pair of corresponding points in object space in the case of two images (a) and unambiguous intersection of three corresponding points in object space in the case of three images (or more)(b)

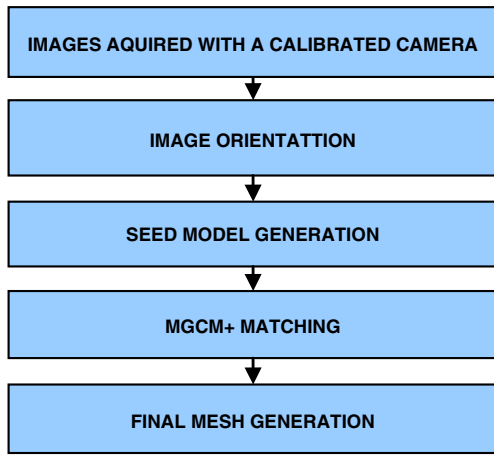


Fig. 2 Workflow of the whole procedure for rock slope surface reconstruction

(NCC) that requires a higher similarity between image contents. Performances of LSM were investigated in Förstner (1986), Förstner and Gülch (1987) and Baltsavias (1991) showing a sub-pixel accuracy in laboratory tests up to 1/20 pixel size. On the other hand, as the algorithm works on the basis of the radiometric content of a couple of images, LSM is highly error prone in the case of repetitive patterns. As can be seen in Fig. 1a, both rays projecting two candidate corresponding points p_0 on the reference image and p_1 on the ‘slave’ must intersect at the same point P in ‘object’ space. Rays O_0p_0 and O_1p_1 are coplanar and define plane π_{01} . The problem is that, as the position of P is still unknown, any other point p'_1 on the ‘slave’ image that belongs to the plane π_{01} , also corresponds to a ray $O_1p'_1$ which intersects line O_0p_0 , but in the wrong position in ‘object’ space (P'). The common place of these points on the ‘slave’ image is termed as *epipolar line*. To overcome this ambiguity, the use of only two images is not sufficient, but at least a third one needs to be introduced.

For this reason, *multi-photo geometrically constrained matching* (MGCM) proposed in Grün and Baltsavias (1988) combines the intensity observations in the nearby of each point to the collinearity condition. In Fig. 1b the presence of

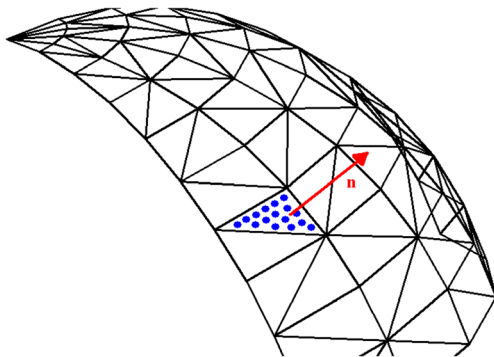


Fig. 3 Definition of starting points for MGCM+ on the TIN structure of the ‘seed’ model

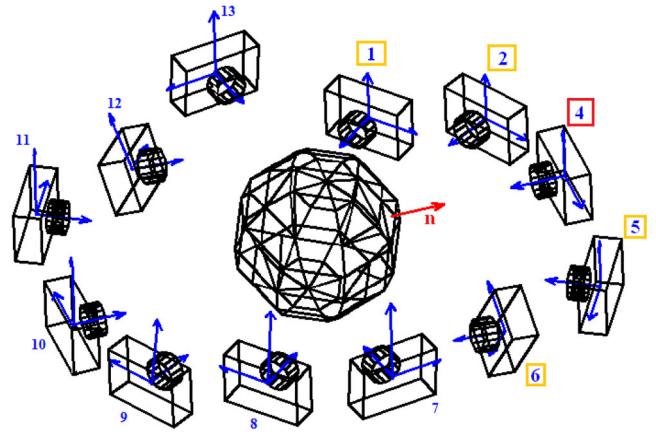


Fig. 4 Example on the selection of the reference and ‘slave’ images per each facet of the ‘seed’ model; the image ‘4’ is selected as reference, while images with label number bordered in yellow are ‘slaves’

a further ‘slave’ image adds a further constraint to the problem and enforces all three projective rays to intersect at the correct point P in ‘object’ space. Any error in the measurement of a corresponding position on any ‘slave’ images will result in a different point in space. Basically, the intensity-based equations in MGCM are written on the basis of a single channel. Today RGB images are generally used, requiring a preliminary transformation into monochromatic images. This is done by computing a combination of RGB channels, or by picking up one channel only (usually the green one if digital sensors are based on the Bayer filter—see Barazzetti and Scaioni 2009).

The matching technique adopted in this research has been termed as MGCM+(Previtali et al. 2011), because it may be considered as an improvement of the original MGCM algorithm where more criteria for selecting the best images for the reconstruction of each portion of the object have been introduced.

In CV field great attention in the recent years has been paid to Semi-Global Matching (SGM), see Hirschmüller (2008). SGM method performs pixel wise matching based on Mutual Information (MI) and the approximation of a global smoothness constraint. In particular, the matching cost for a base image is calculated pixel wise by considering pixel intensities and suspected correspondences. The cost calculation is performed by means of MI which is insensitive to recording and illumination changes. However, pixel wise cost calculation is generally ambiguous and wrong matches can easily have a lower cost than correct ones. For this reason a smoothness constraint is enforced by penalizing changes of neighboring disparities and a final pixel wise energy term can be formulated as the sum of the different cost terms. In this way, the stereo-matching problem can be formulated as finding the disparity image D that minimizes the total energy. This minimization is performed by aggregating, for each pixel p , one-dimensional minimum costs path that ends in p from all directions equally.

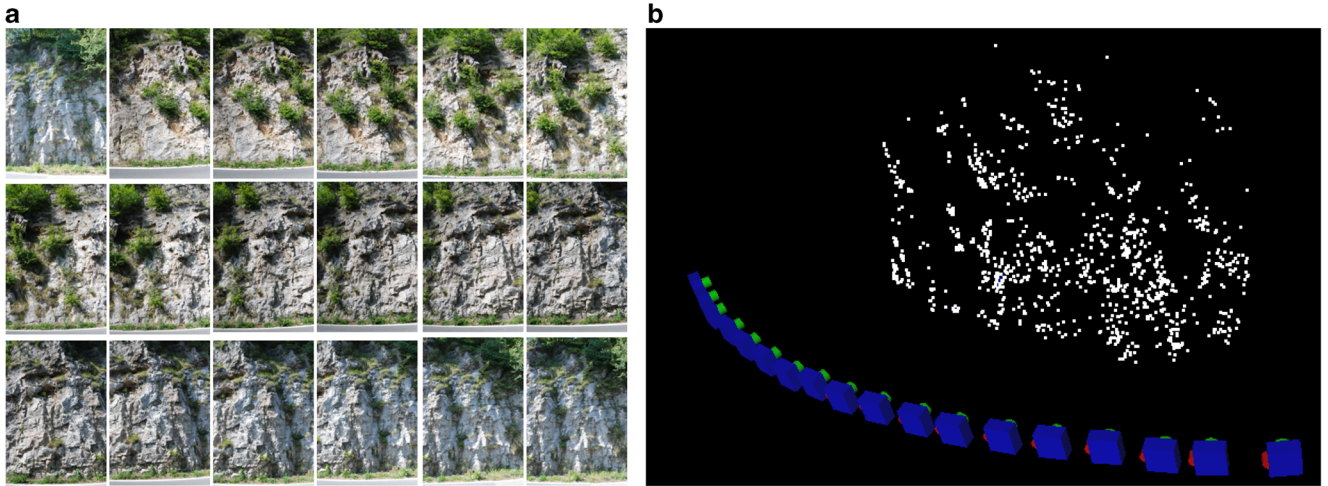


Fig. 5 Images used for the reconstruction of the rock face in Esino Lario (a), scheme of camera poses and extracted tie points for image orientation (b)

SMG matching works on single image pair and does not exploit the presence of a higher number of images during the matching phase. The problem of mismatches is coped with by using the smoothing approach, but this may result in a low-pass filtering. In the areas with overlapping images, the reconstructed point cloud needs to be merged together. In the MGCM concept, the image redundancy is exploited since the beginning to increase the reliability of the reconstructed points. No filtering step is applied and consequently MGCM may preserve more details in the reconstructed model. The use of MGCM has been preferred when precision and reliability of the reconstructed model are primary characteristics, as in the applications investigated here.

The reconstruction procedure

In this section the proposed reconstruction procedure of 3D objects by using high resolution images is summarized. Due to the theoretical complexity of MGCM+ algorithm, the reader is addressed to Previtali et al. (2011) for technical details and for background information.

In the developed LSM implementation the geometric model adopted for patch warping is based on an affine transformation. Radiometric terms (usually two linear terms are implemented) are not considered in the LS minimization to avoid

Table 2 Bundle adjustment statistics for ‘Esino Lario’ dataset

	Esino Lario (23 images)	
	ATiPe	PhotoModeler
3D points	1,273	3,925
σ_0 (pix)	0.465	0.513
RMS (pix)	0.493	0.504
Check point RMSE (mm)	1.7	2.1

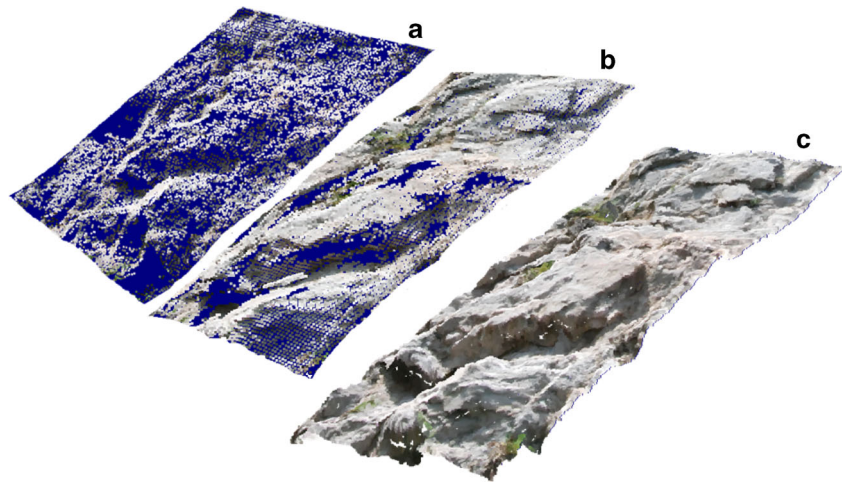
over-parameterization of the problem, but a radiometric equalization between matching windows on the reference and ‘slave’ images is applied before any iterations. As can be seen in the flowchart in Fig. 2, two pre-requisites are needed for MGCM+: (i) the knowledge of camera calibration and EO parameters of all images; (ii) a set of approximate values both for image and object coordinates. The meaning of pre-requisite (i) is obvious: position and attitude of images in space should be known as best as possible to improve the determination of surface points by using 3D intersection.

Approximate coordinates for every candidate point on both the reference and the ‘slave’ images are due to the fact that the mathematical problem is nonlinear and its solution by means of linearized LS requires approximate good values. A rough object model (‘seed’ model) is usually used to this purpose. If not already available from previous surveys, a common approach is to apply a pair wise matching technique (e.g., LSM or NCC) to obtain an initial model to be refined later by using MGCM+. In this implementation an alternative solution has been followed, based on the fact that a large number of tie points are usually extracted by automatic image orientation procedures. These points may be interpolated using a *Triangular Irregular Network* (TIN) structure so that they may be used to define a ‘seed’ model without any additional effort.

On each facet of the triangulated ‘seed’ model (Fig. 3) a regular grid is established, whose step is approximately the desired point density in the final 3D model. These grid points on the TIN structure represent the approximate positions for the points in the final 3D point cloud. Back-projecting these points onto the images yield the approximate positions of the homologous points.

Another aspect which has been investigated in the implementation of MGCM+ is the criterion to select images to be matched together. In many cases, MGCM has been implemented with aerial images. In such case, any image is selected to be the reference image at turn, and next images in the

Fig. 6 Comparison between models: Original ‘seed’ model (a), 7×7 cm inter-distance model (b), 2×2 cm inter-distance final model (c)



regular strip are used as ‘slaves.’ This choice is acceptable in mapping applications, where the surface can be represented by a 2.5D model. In close-range photogrammetry this simplification does not generally hold any more, because the image network may be more complex (see example in next section). In addition, in the case more than 3–4 images overlap over the same area, the use of all of them is pointless and may result in blunders due to occlusions. For these reasons an optimization in the selection of images to be matched is needed. Concerning the selection of the reference image, for each facet of the TIN surface the local normal vector n is defined (see Fig. 4). The reference image is the one whose normal vector is closer to the surface normal direction of the considered surface. In this way the definition of the reference image may change from one mesh triangle to another of the ‘seed’ model.

The second problem concerns the choice of the actual ‘slave’ images to be effectively used. This optimization is still performed by exploiting the ‘seed’ model. In particular, only the images whose normal vectors form an angle lower than 90° with the local surface normal are used (Fig. 4). Moreover, in many cases the perspective deformations between different images can be so large that the geometric transformation model (usually an affine) incorporated in MGCM+ could not compensate for them. Indeed, the estimation of all parameters

in MGCM+ is performed by using linearized LS. Linearization is based on approximate values for all unknowns. In the case of the affine parameters, a reasonable guess may be estimated only if the perspective differences are not too large. To this aim, all selected ‘slaves’ are analyzed and only those for which MGCM+ can provide reliable results are effectively processed. In particular each triangle in the ‘seed’ model is back-projected onto the reference and all potential ‘slave’ images. Two shape parameters are evaluated: the area of the triangles and their angular variations. If the area of a back-projected triangle on a potential ‘slave’ is less than 50 % of the area of the related triangle in the reference image, or the angular variation of the projected triangle exceed 40 %, the image is not considered for processing of points on that mesh of the TIN model.

Experimental applications

In this section some cases in which the 3D reconstruction procedure has been tested are presented and discussed. A quite wide range of different situations has been covered to assess the flexibility of the method. In all the examples a calibrated camera has been used. Exterior orientation has been computed

Fig. 7 The final point cloud obtained for the rock face in Esino Lario textured with images

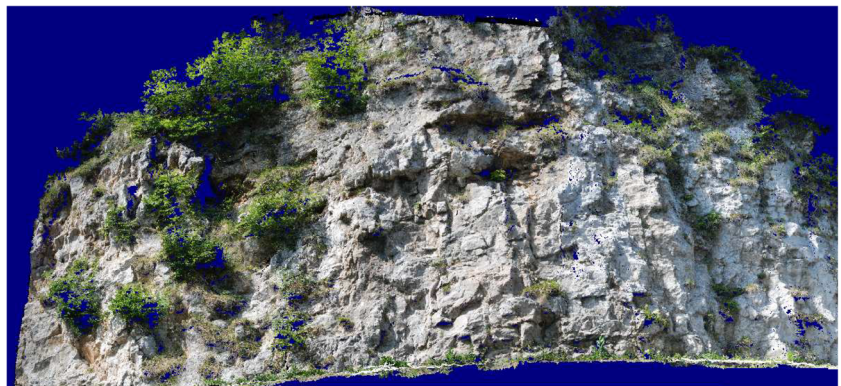
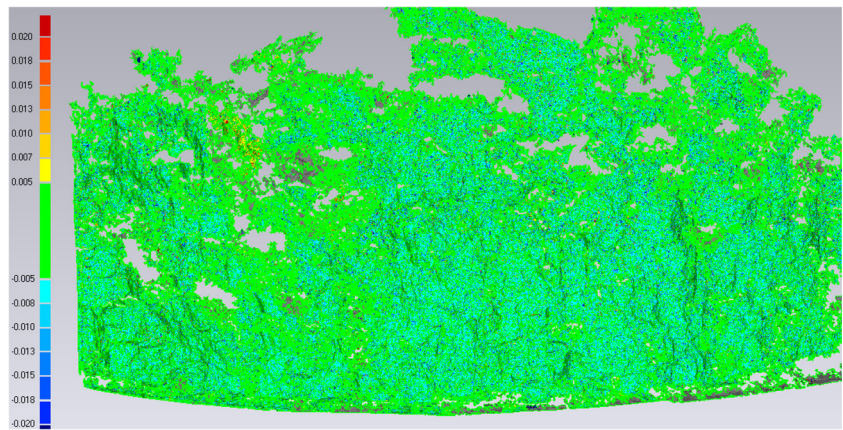


Fig. 8 ICP comparison between ‘photogrammetric’ and ‘TLS’ (method ‘A’) models for the reconstructed rock face in Esino Lario; the color scale ranges from +2 to -2 cm



using the automatic procedure ATiPE for tie point extraction followed by a rigorous bundle adjustment. Due to the high number of tie points extracted (always more than 1000 points per project) and their uniform distribution on the slope surface, these has been directly used to derive the ‘seed’ models for the MCGM+matching algorithm.

Rock face in esino lario

The first site is located in the Italian Pre-Alpine region, just close to a county road in the municipality of Esino Lario (Lecco, Italy). Here a rock face was surveyed in order to evaluate the risk of rock falls (Longoni et al. 2012). A TLS survey, performed by a Riegl LSM-Z420i laser scanner, was also available to validate the photogrammetric result (Scaioni et al. 2013). The slope was approximately 20 m wide and 10 m high. An important aspect to be noticed was the presence of vegetation on the cliff. For photogrammetric surveying, problems connected to image matching on areas covered by vegetation are well known and these could lead to the incomplete reconstruction of these regions. However, to obtain a digital model of the cliff, vegetation should be generally filtered out to obtain the bare rock surface (Alba et al. 2011; Pirotti et al. 2013b). The alignment of laser scans among them and with respect to the photogrammetric point cloud was carried out by

using a set of retro-reflective targets as GCP’s. Their position was measured by theodolite Leica TS30. For the photogrammetric survey a block of 18 images (Fig. 5a) were captured using a Nikon D80 camera (Table 1). In this case image orientation has also been tackled by using the PhotoModeler® 2013 module for *targetless* automatic image orientation (SmartPoint®). Statistics on the EO are presented in Table 2; a scheme of camera poses is shown in Fig. 6b. As can be seen from Table 2, PhotoModeler® extracted a far larger number of tie points than the ones obtained with ATiPe. This is partially due to the fact that the two software packages rely on different feature extraction algorithm: SIFT (Löwe 2004) is implemented in PhotoModeler® and FAST (Rosten and Drummond 2006) in ATiPe. In addition, in ATiPe a procedure for regularization of tie point distribution is implemented, which keeps only those with higher multiplicity. Indeed, a regular and homogeneous distribution of multiple tie points (i.e., tie points measured on at least 3–4 images) may provide a good result, as witnessed by the smaller sigma naught obtained with ATiPe. A further increase of the total number of tie points does not correspond to an increased accuracy, but only in a larger computational burden.

MGCM+algorithm was run in two steps. First, a coarser TIN model was build imposing a 7×7 cm grid among points on the approximate mesh, whose average resolution was

Table 3 Comparison results for all case studies; discrepancies are presented in terms of mean and standard deviation for both methods ‘A’ and ‘B’

Statistic on discrepancies between rock faces reconstructed with different techniques

	Esino (TLS surveying)			San Martino (photogrammetric surveying/LPS-eATE)			Tartano (photogrammetric surveying/LPS-eATE)		
	Mean (mm)	Standard deviation (mm)	RMSE (mm)	Mean (mm)	Standard deviation (mm)	RMSE (mm)	Mean (mm)	Standard deviation (mm)	RMSE (mm)
Method ‘A’	8	5	4	91	86	84	11	18	13
Method ‘B’	5	3	4	89	57	48	10	15	12

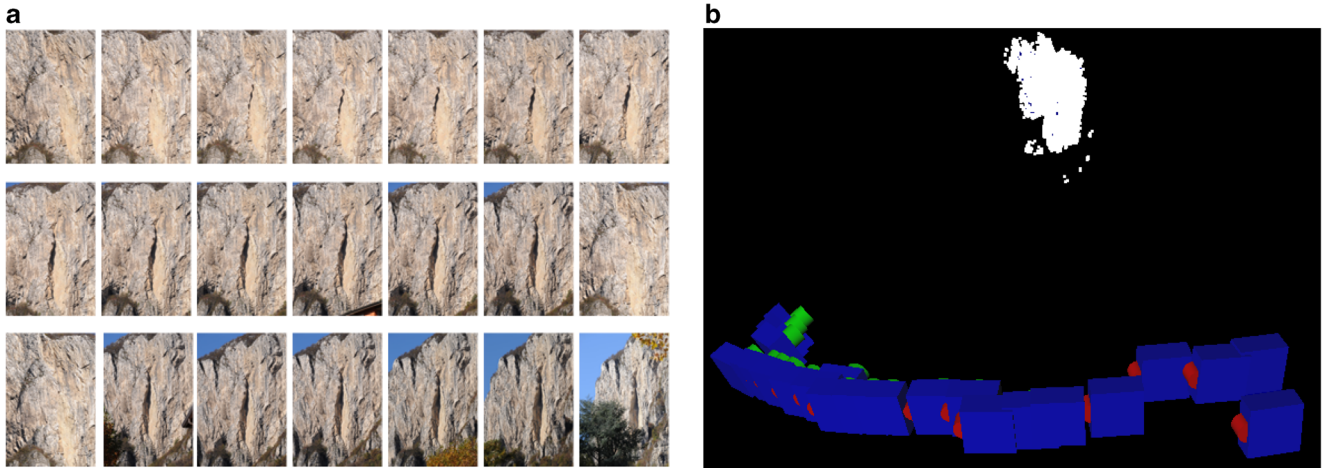


Fig 9 Images used for the San Martino rock face reconstruction (a) and scheme of camera poses and extracted tie points by using ATiPe (b)

20×20 cm. This resulted in a point extracted every 8×8 pixels on the images. Secondly, such a model was used as ‘seed’ model, and a 2×2 cm grid among points was selected to generate the final 3D model. In Fig. 6 a comparison between the different models is presented while in Fig. 7 the final point cloud of the entire rock face is shown.

To validate the results a comparison between ‘photogrammetric’ and ‘TLS’ point clouds was performed. In particular, two different methods were used for comparison. Method ‘A’ was based on the preliminary triangulation of both point clouds. The obtained TIN structures are then compared by using the *Iterative Closest Point* surface matching algorithm (Besl and McKay 1992). Figure 8 shows the visual result of this comparison on the whole cliff. Method ‘B’ was based on the construction of two raster *digital elevation models* (DEM’s) starting from the point clouds and then evaluating the difference between them. This second comparison evaluates only the off-plane displacements of the rock cliff. Results for both comparisons are presented in Table 3. Since the point precision of TLS model ranged in the order of 10 mm, both outcomes proved the metric validity of the photogrammetric point cloud, which however showed a satisfying completeness.

San Martino rock face

The second application was the San Martino rock face in Lecco (Italy). In this case a geometric model of the cliff was needed in order to design the deployment of a sensor network for monitoring purpose. The rock cliff is approximately 120 m wide and 150 m high and, moreover, the investigated area is located at 100 m from the slope toe. In such a case a TLS surveying was not feasible due to logistical grounds, as the closer possible standpoint is far from the cliff (more than 800 m). A very-long range laser scanner was not available at that time. For such a reason the photogrammetric survey could

be considered more appropriate. In order to cover the full cliff and to guarantee an adequate level of detail, a careful design of the photogrammetric network was needed (Fig. 9b). In particular a calibrated Nikon D700 with a 180 mm lens was employed to acquire 23 images (Fig. 9a), while the average distance from the camera stations and the rock cliff was about 700 m.

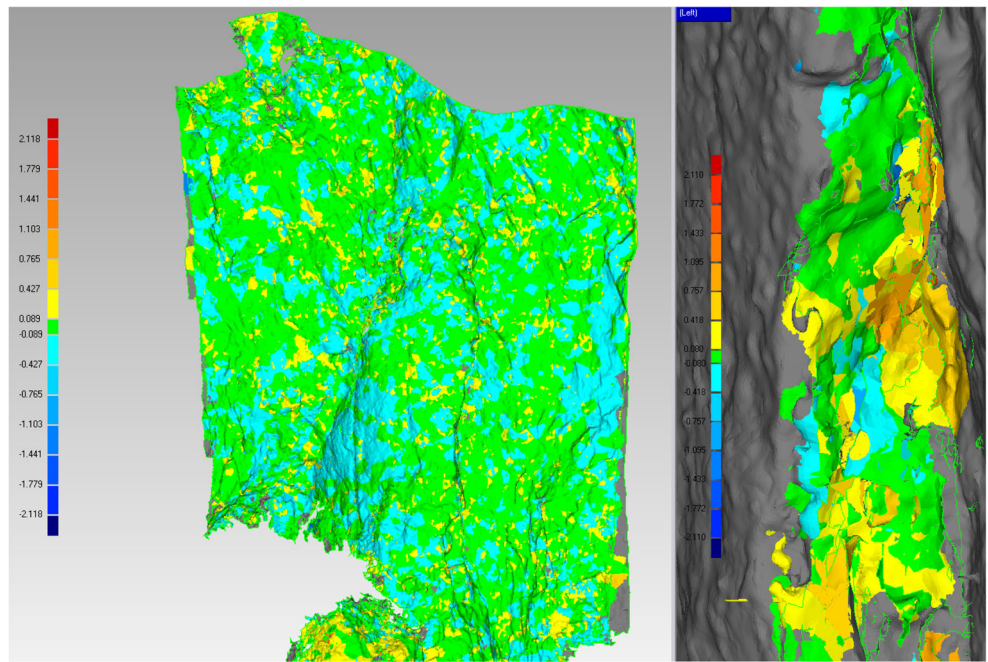
The statistics of EO obtained using ATiPe software are presented in Table 4. In this case, the GRS was setup by measuring the position of a few photogrammetric stations with a GPS receiver and no statistics about check point RMSE are available, unfortunately.

In this case, the assessment of the results was accomplished by comparing the ‘photogrammetric’ point cloud obtained from MGCM+ with one achieved with the commercial photogrammetric software LPS-eATE®. In spite of the fact this software was developed for aerial mapping purposes, it worked out well with this dataset where the shape of the rock surface could be split into several 2.5D regions. The same comparison methods adopted for the previous example were applied here (results in Table 3). In Fig. 10 the discrepancies obtained with method ‘A’ are shown for the full investigated area. The area showing the higher discrepancy is a recess in the cliff generated by a previous rock fall, which cannot be easily modelled in a 2.5D way. Consequently, the reference model obtained with LPS-eATE® is not reliable here, whilst the proposed method could successfully handle the entire 3D surface.

Table 4 Bundle adjustment statistics for ‘San Martino rock face’ dataset

	San Martino–ATiPe (23 images)
3D points	9,615
σ_0 (pix)	0.328
RMS (pix)	0.378

Fig. 10 ICP comparison (method 'A') between surfaces obtained from photogrammetric approaches based on MGCM+ and LPS-eATE® for the 'San Martino rock face'; the color scale ranges from +2.1 to -2.1 m



Tartano slope

The third application presented here concerns the measurement of large debris movements along time in the Tartano Valley, located in the Italian Alpine region (Sondrio). The land erosion in this valley can cause the sediment transport of debris into the Tartano River, turning out into serious problems in the case of intense rainfalls. For this reason the process was monitored in order to understand its magnitude. The slope to be observed is 240 m long and 130 m wide. In this case, a

geodetic network was established to setup a stable GRS to compare data gathered at three different epochs (July 2010, August 2010 and July 2011). A set of GCP's was placed on the slope and their positions measured with a theodolite.

At each epoch 13 images (Fig. 11a) were acquired by using a Nikon D700 equipped with a 90 mm lens (Table 1). The EO was independently computed at each epoch by using ATiPe; statistics are shown in Table 5.

Even in this case the final point clouds obtained at each observation epochs were compared to the one derived using

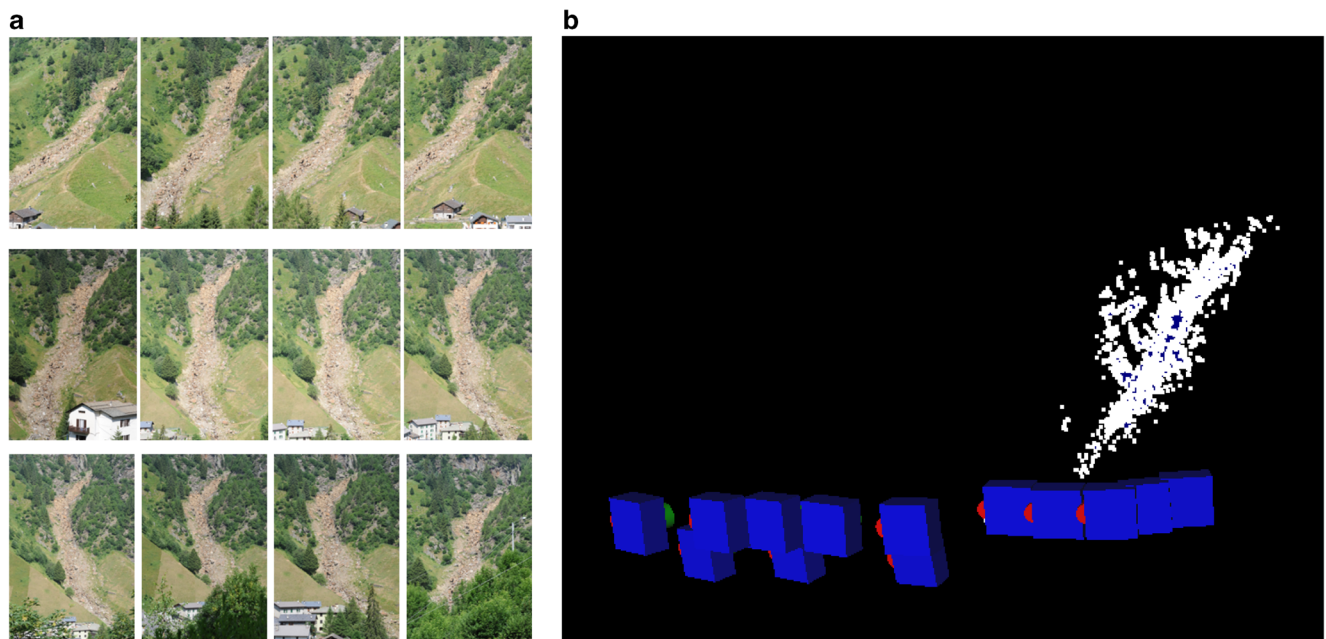


Fig. 11 Images used for reconstruction of the slope in Tartano Valley at epoch 1(a) and scheme of camera poses and extracted tie points at epoch 1(b)

Table 5 Bundle adjustment statistics for ‘Tartano slope’ dataset

	Tartano–ATiPe (12 images)		
	15/7/2010	3/8/2010	10/7/2011
3D points	2972	2965	5345
σ_0 (pix)	0.610	0.619	0.611
RMS (pix)	0.748	0.778	0.749
Check point RMSE (mm)	9.2	9.9	9.6

LPS-eATE[®], because a laser scanning surveying was not available. In such a case however the results obtained by using this software presents some evident blunders in the lower part of the valley flank. After manually editing the point cloud to remove unreliable areas from the reference point cloud, both assessment methods ‘A’ and ‘B’ were applied (results are in Table 3).

The evaluation of differences in the slope surface geometry acquired at different epochs were also carried out in the same manner. Results are summarized in Fig. 12 for the comparison with method ‘A’.

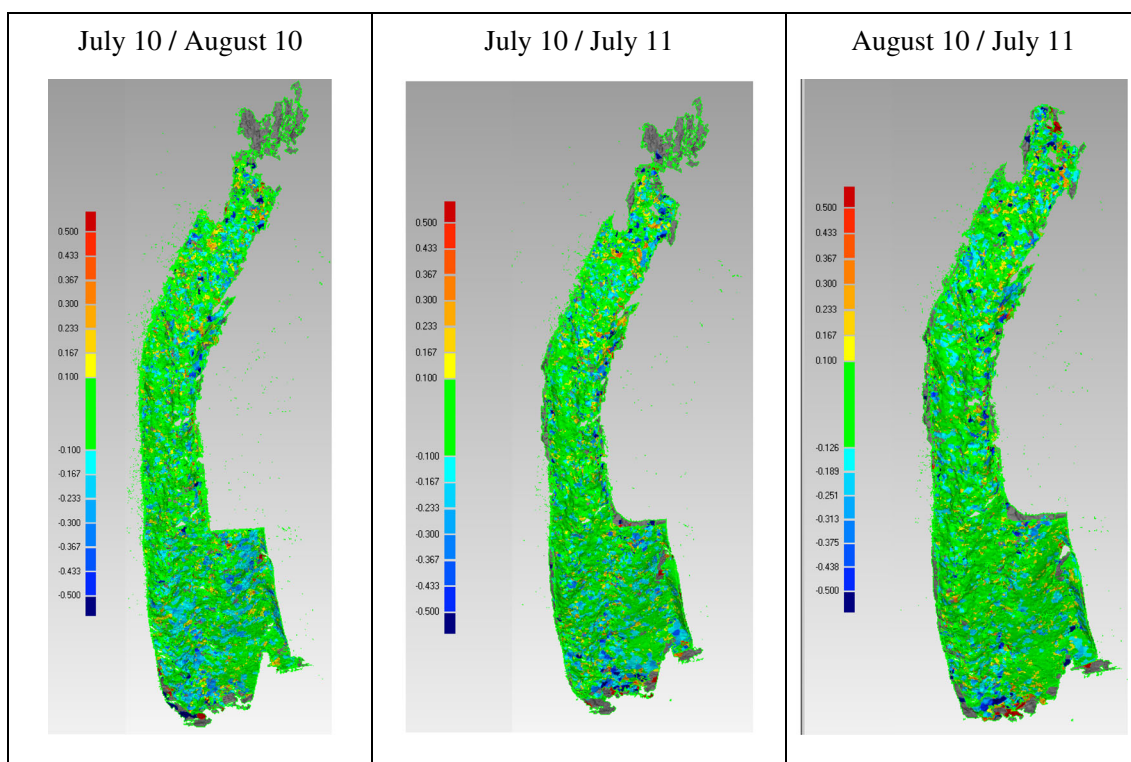
In all cases no significant global displacements of the slope were found. However, focusing on some details, some small changes can be observed. For example, in Fig. 13 one of these displacements is highlighted between epochs 1 and 3. On the other hand, the displacement seems to be confirmed from the

comparison between epochs 2 and 3, while no change is detected between epochs 1 and 2. Also a visual inspection seems to confirm the results. However because of the high sediment transport in this area, it is generally very difficult to detect any changes.

Conclusions

Several techniques are today available and may be integrated in order to reconstruct the geometry of rock and ground slopes. In particular, in this paper a photogrammetric procedure for the reconstruction of topography of slopes and cliffs has been presented. The operational workflow is completely automated, starting from camera calibration and image orientation to the generation of a dense point cloud and its interpolation. The only manual phase consists in data acquisition.

Two important aspects of this research are the implementation automatic procedures for images orientation and surface reconstruction. The former is based on scientific software for automatic exterior orientation of the images (ATiPe), which may be retained as representative of the state-of-the-art techniques, as demonstrated by the comparison with commercial software (PhotoModeler[®]). The latter is afforded by using a multi-photo matching algorithm (MGCM+) based on modified Multiphoto Geometrically Constrained Matching (MGCM) technique. Although this is an ‘old’ algorithm, it is

**Fig. 12** ICP comparison (method ‘A’) between different epochs for the slope in Tartano Valley; the color scale ranges from +0.5 to –0.5 m

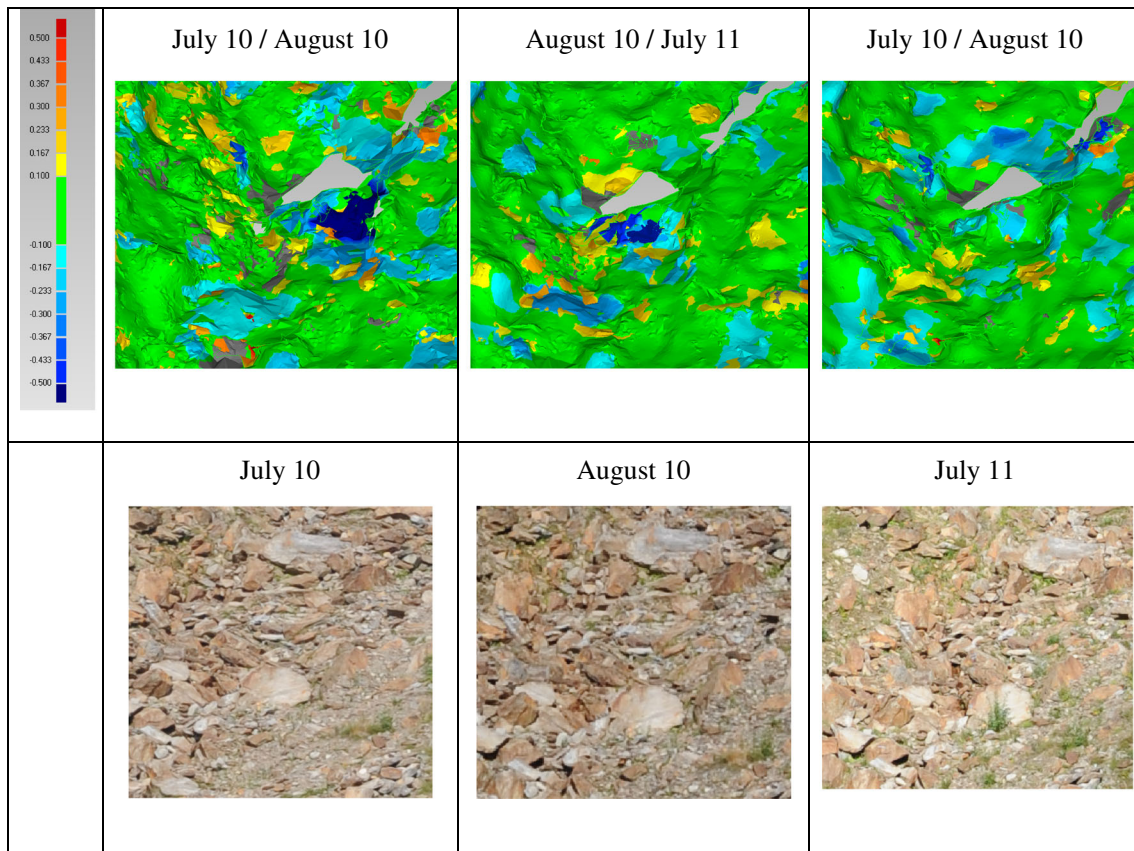


Fig. 13 Detected displacement of a big rock which can be seen from the comparison between different epochs' results (on the top line). On the bottom, images are reported to prove the detected changes

still one of the most precise and reliable methods for dense matching. Some problems related to the standard MGCM implementation were overcome here. More precisely, a particular attention was paid to the selection of images to serve as reference and 'slaves' at their own turns. Further developments are still required to reduce the CPU time, being the implementation at GPU level one viable solution.

In the experimental section, three applications of the developed photogrammetric procedure for the reconstruction of three different mountain slopes were presented. The first case study (a small rock face in Esino Lario, Italy) demonstrated that in the case the distance between the camera stations and the target object is properly selected, a similar precision to the one obtainable with a terrestrial laser scanning (TLS) can be achieved. Indeed, by comparing point clouds coming from TLS and photogrammetry, discrepancies were found in accordance with the laser scanning measurement uncertainty. In the second case study ('San Martino' rock face, Italy), the distance from the potential instrument standpoints was out of the maximum operational range of the available laser scanner. Consequently the photogrammetric method was used as the only possible solution, but also in this case the results in terms of completeness of the final point 3D model and precision of reconstructed points were enough for the following

application. The comparison of the photogrammetric point cloud to the one processed by another efficient matching technique which is commonly adopted in mapping projects (LPS-eATE[®]) revealed a similar output but a better completeness. In the third application (a slope in Tartano Valley, Italy), the challenging problem of change detection was tackled. In particular, by repeating the photogrammetric survey at three observation epochs and by comparing the obtained point clouds, the general status of soil weathering and also the movement of large rock blocks could be highlighted. Even though the developed strategy gave satisfactory results in applications presented here, a major limitation of the adopted MGCM+ algorithm is the cost in terms of computational time. Indeed, for 'San Martino' dataset the increase of model resolution from a 7×7 cm grid up to a 2×2 cm grid resulted in a growth of processing time from minutes to hours. Alternative solutions like Semi-Global Matching may outperform MGCM+ in terms of processing time. On the other hand, MGCM+ is based on multiple, redundant observations and may provide more reliable results. In the applications carried out in this research, the combination of ATiPe and MGCM+ furnished good quality outputs for the subsequent interpretation or processing tasks. A more comprehensive experimentation of diverse matching technique with some benchmarking

datasets that may be representative of real slopes and cliffs needs to be afforded in future research.

A last observation concerns the comparison between the photogrammetric method and TLS surveying. Both techniques provide the same output, i.e., a point cloud describing the topographic surface of the target slope with sufficient point density and precision. Images may also be used for texturing the point cloud, but this option is today quite common in up-to-date laser scanners thanks to an integrated camera. Laser scanners may provide a point cloud in a straightforward manner, not requiring the sense image matching phase for surface reconstruction. On the other hand, automatic image orientation techniques have drastically simplified this task, whose burden is now comparable to the one related to scan registration. In both cases, geo-referencing into a ground reference system require a set of ground control points. The developed image-based procedure, as all similar strategies, may fail in the case of rock faces with large homogenous areas. In such cases, active sensors as laser scanners do not suffer from this problem. This analysis outlines that laser scanners should be generally the best solution to cope with topographic surveys for engineering geology applications. Unfortunately, laser scanners are still expensive and cumbersome. Photogrammetric may be a useful alternative to TLS right when the user has to cope with these limitations. Indeed the total cost of the photogrammetric equipment is quite small (below 5000 euros), while cameras may be carried almost everywhere with more easy. In addition, digital cameras may be installed on small UAV's to allow reaching non-directly accessible areas. This option cannot be provided yet by modern laser scanners. These considerations make the photogrammetric process an important alternative or integration to TLS to extend the chance to reconstruct the 3D geometry of a large number of slopes.

References

- Abellán A, Vilaplana JM, Martínez J (2006) Application of a long-range terrestrial laser scanner to a detailed rockfall study at vall de núria (Eastern Pyrenees, Spain). *Eng Geol* 88(3–4):136–148
- Abellán A, Jaboyedoff M, Oppikofer T, Vilaplana JM (2009) Detection of millimetric deformation using a terrestrial laser scanner: experiment and application to a rockfall event. *Nat Hazards Earth Syst Sci* 9(2): 365–372
- Abidin H, Andreas H, Gamal M, Sadarviana V, Darmawan D, Surono Hendrasto M, Suganda O (2007) Studying landslide displacements in the ciloto area (Indonesia) using GPS surveys. *J Spat Sci* 52(1):55–63
- Agarwal S, Snavely N, Simon I, Seitz SM, Szeliski R (2009) Building rome in a day. *Commun ACM* 54(10):105–112
- Agliardi F, Crosta G (2003) High resolution three-dimensional numerical modelling of rockfalls. *Int J Rock Mech Min Sci* 40(4):455–71
- Alba MI, Barazzetti L, Roncoroni F, Scaioni M (2011) Filtering vegetation from terrestrial point clouds with low-cost near infrared cameras. *Ital J Remote Sens* 43:55–75
- Baltsavias EP (1991) Multiphoto geometrically constrained matching. Ph.D. thesis No. 9561, Mitteilungen Nr. 49, Institute of Geodesy and Photogrammetry, ETH Zurich, Switzerland. 221 pages.
- Barazzetti L, Scaioni M (2009) Crack measurement: development, testing and applications of an automatic image-based algorithm. *ISPRS J Photogramm Remote Sens* 64(3):285–296
- Barazzetti L, Remondino F, Scaioni M (2010) Orientation and 3D modelling from markerless terrestrial images: combining accuracy with automation. *Photogramm Rec* 25(132):356–381
- Barazzetti L, Forlani G, Remondino F, Roncella R and Scaioni M (2011) Experiences and achievements in automated image sequence orientation for close-range photogrammetric projects. In: Proc. Int. Conf. “Videometrics, Range Imaging, and Applications XI”, 23–26 May, Munich (Germany), Proc. of SPIE, Vol. 8085, paper No. 80850F, 13 pages.
- Barla G, Antolini F, Barla M, Mensi E, Piovano G (2010) Monitoring of the Beauregard landslide (aosta valley, Italy) using advanced and conventional techniques. *Eng Geol* 116(3–4):218–235
- Besl PJ, McKay ND (1992) A method for registration of 3-D shapes. *IEEE Trans Pattern Anal Mach Intell* 14(2):239–256
- Duncan CW, Norman IN (1996) Stabilization of rock slopes. In: Turner AK, Schuster RL (eds) *Landslides investigations and mitigation, special report 247*. Transportation Research Board, National Research Council, Washington, pp 474–506
- Eisenbeiss H, Sauerbier M (2011) Investigation of UAV systems and flight modes for photogrammetric applications. *Photogramm Rec* 26(136):400–421
- Feng Q, Sjogren P, Stephansson O, Jing L (2001) Measuring fracture orientation at exposed rock faces by using a non-reflector total station. *Eng Geol* 59(1–2):133–146
- Ferrero AM, Forlani G, Roncella R, Voyat HI (2009) Advanced geostuctural survey methods applied to rock mass characterization. *Rock Mech Rock Eng* 42(4):631–665
- Förstner W (1986) A feature based correspondence algorithm for image matching. *Int Arch Photogramm Remote Sens* 26(3):150–166
- Förstner W, Gülch E (1987) A fast operator for detection and precise location of distinct points, corners and centres of circular features. In *ISPRS Intercommission Workshop, Interlaken*, pp 281–305
- Fraser CS (2013) Automatic camera calibration in close range photogrammetry. *Photogramm Eng Remote Sens* 79(4):381–388
- Fraser CS, Cronk S (2009) A hybrid measurement approach for close-range photogrammetry. *ISPRS J Photogramm Remote Sens* 64(3): 328–333
- Furukawa Y, Ponce J (2007) Accurate, dense, and robust multi-view stereopsis. *IEEE Trans Pattern Analysis Mach Intell* 32(8):1362–1376
- Gao J, Liu C, Wang J, Li Z, Meng X (2011) A new method for mining deformation monitoring with GPS-RTK. *Trans Nonferrous Metals Soc China* 21:659–664
- García-Sellés D, Falivene O, Arbués P, Gratacos O, Tavani S, Muñoz J (2011) Supervised identification and reconstruction of near-planar geological surfaces from terrestrial laser scanning. *Comput Geosci* 37(10):1584–1594
- Gigli G, Casagli N (2011) Semi-automatic extraction of rock mass structural data from high resolution LIDAR point clouds. *Int J Rock Mech Min Sci* 48(2):187–198
- Grün A (1985) Adaptive least square correlation—a powerful image matching technique. *Afr J Photogrammetry Remote Sens Cartog* 14(3):175–187
- Grün A, Baltsavias EP (1988) Geometrically constrained multiphoto matching. *Photogramm Eng Remote Sens* 54(5):633–641
- Grün A (2012) Development and status of image matching in photogrammetry. *Photogramm Rec* 27:36–57
- Heritage GL, Large ARG (2009) *Laser scanning for the environmental sciences*. Wiley, UK

- Hirschmuller H (2008) Stereo processing by semiglobal matching and mutual information. *IEEE Trans Pattern Analysis Mach Intell* 30(2): 328–341
- Jaboyedoff M, Oppikofer T, Abellán A, Derron MH, Loye A, Metzger R, Pedrazzini A (2012) Use of LIDAR in landslide investigations: a review. *Nat Hazards* 61:5–28
- Joyce KE, Belliss SE, Samsonov SV, McNeill SJ, Glassey PJ (2009) A review of the status of satellite remote sensing and image processing techniques for mapping natural hazards and disasters. *Prog Phys Geogr* 33(2):183–207
- Kasperski J, Delacourt C, Allemand P, Potherat P, Jaud M, Varrel E (2010) Application of a terrestrial laser scanner (TLS) to the study of the Séchilienne Landslide (Isère, France). *Remote Sens* 2(12): 2785–2802
- Kemeny J, Post R (2003) Estimating three-dimensional rock discontinuity orientation from digital images of fracture traces. *Compt Rendus Geosci* 29(1):65–77
- Kraus K (2007) *Photogrammetry, Geometry from images and laser scans*. Walter de Gruyter, Germany, p 459
- Lemy F, Hadjigeorgiou J (2003) Discontinuity trace map construction using photographs of rock exposures. *Int J Rock Mech Min Sci* 40(6):903–917
- Longoni L, Arosio D, Scaioni M, Papini M, Zanzi L, Roncella R, Brambilla D (2012) Surface and subsurface non-invasive investigations to improve the characterization of a fractured rock mass. *J Geophys Eng* 9:461–472
- Löwe DG (2004) Distinctive image features from scale-invariant keypoints. *Int J Comput Vis* 60:91–110
- Luhmann T (2011) 3D imaging—how to achieve highest accuracy. In *Videometrics, Range Imaging, and Applications XI*, vol. 8085 of *Proceedings of SPIE*, pp. 1–11, 808502.
- Martha TR, Kerle N, Jetten V, Van Westen CJ, Kumar KV (2010) Spatial and morphometric properties of landslides for semi-automatic detection using object-oriented methods. *Geomorphology* 116(1–2):24–36
- Mora P, Baldi P, Casula G, Fabris M, Ghirotti M, Mazzini E, Pesci A (2003) Global positioning systems and digital photogrammetry for the monitoring of mass movements: application to the Ca' di Malta landslide (Northern Apennines, Italy). *Eng Geol* 68(1–2):103–121
- Nex F, Remondino F (2014) UAV for 3D mapping applications: a review. *Appl Geomatics* 6(1):1–15
- Nguyen HT, Fernandez-Steeger TM, Wiatr T, Rodrigues D, Azzam R (2011) Use of terrestrial laser scanning for engineering geological applications on volcanic rock slopes—an example from Madeira island (Portugal). *Nat Hazards Earth Syst Sci* 11(3):807–817
- Oppikofer T, Jaboyedoff M, Blikra L, Derron MH, Metzger R (2009) Characterization and monitoring of the aknes rockslide using terrestrial laser scanning. *Nat Hazards Earth Syst Sci* 9(3):1003–1019
- Pierrot Deseilligny M and Clery I (2011) APERO, an open source bundle adjustment software for automatic calibration and orientation of set of images. *Int. Archives of Photogrammetry, Remote Sensing and Spatial Information Sciences*, 38 (5/W 16), pp. 269–277, on CD-ROM. ISPRS International Workshop 3D ARCH 2011, Trento, Italy, 2–4 March 2011.
- Pirotti F, Guarnieri A, Vettore A (2013a) State of the art of ground and aerial laser scanning technologies for high-resolution topography of the earth surface. *Eur Remote Sens* 46:66–78
- Pirotti F, Guarnieri A, Vettore A (2013b) Ground filtering and vegetation mapping using multi-return terrestrial laser scanning. *ISPRS J Photogramm Remote Sens* 76:56–63
- Previtali M, Barazzetti L and Scaioni M (2011) Multi-step and multi-photo matching for accurate 3D reconstruction. *International Archives of Photogrammetry, Remote Sensing and Spatial Information Sciences, Photogrammetric Image Analysis* 38(3/W22):103–108.
- Prokop A, Panholzer H (2009) Assessing the capability of terrestrial laser scanning for monitoring slow moving landslides. *Nat Hazards Earth Syst Sci* 9:1921–1928
- Reid T, Harrison J (2000) A semi-automated methodology for discontinuity trace detection in digital images of rock mass exposures. *Int J Rock Mech Min Sci* 37(7):1073–1089
- Rosten E, Drummond T (2006) *Machine learning for high-speed corner detection*, *Proceedings of the European conference on computer vision*. Springer Berlin Heidelberg, Graz, pp 430–443
- Salvini R, Francioni M, Riccucci S, Fantozzi P, Bonciani F, Mancini S (2011) Stability analysis of “grotta Delle felci” cliff (Capri island, Italy): structural, engineering–geological, photogrammetric surveys and laser scanning. *Bull Eng Geol Environ* 70(4):549–557
- Scaioni M, Alba M, Giussani A, Roncoroni F (2010) Monitoring of a SFRC retaining structure during placement. *Eur J Environ Civ Eng* 14(4):467–493. doi:10.3166/EJECE.14.467-493
- Scaioni M, Roncella R, Alba MI (2013) Change detection and deformation analysis in point clouds: application to rock face monitoring. *Photogramm Eng Remote Sens* 79(5):441–456
- Schofield W and Breach M (2007) *Engineering Surveying—6th Edition*. Butterworth-Heinemann.
- Shan J, Toth CK (2009) *Topographic laser scanning and ranging. Principles and processing*, Taylor and Francis group. Boca Raton, FL-USA
- Slob S, Van Knapen B, Hack R, Turner K, Kemeny J (2005) Method for automated discontinuity analysis of rock slopes with three-dimensional laser scanning. *Transp Res Rec* 1913:187–194
- Travalletti J, Oppikofer T, Delacourt C, Malet JP, Jaboyedoff M (2008) Monitoring landslide displacements during a controlled rain experiment using a long-range terrestrial laser scanning (TLS). *Int Arch Photogramm Remote Sens Spat Inf Sci* 37(B5):485–490
- Vosselman G, Maas HG (2010) *Airborne and terrestrial laser scanning*. Taylor and Francis Group, Boca Raton
- Yang IT, Park JK, Kim DM (2007) Monitoring the symptoms of landslide using the non-prism total station. *KSCE J Civ Eng* 11(6):293–301